The work in this project is entirely my own, except where specific reference is made.

Candidate Number	36102
College	Keble
Signed	
Date	27th April 2007

Candidate Number: 36102

AO10: SCATTERING BY NON-SPHERICAL PARTICLES

Supervisor: Dr Elisa Carboni

Word Count: 5,203
(excluding references, figures, labels on figures, figure captions, tables and equations)

AO10: SCATTERING BY NON-SPHERICAL PARTICLES

ABSTRACT

Modelling the properties of aerosols present in the troposphere is complicated by many factors, such as their intrinsic irregularity. Using a T-matrix code, this study addressed the non-sphericity of transported desert dust using a pre-computed mixture of water soluble and mineral dust components. The scale of this effect on certain optical properties observed in remote sensing was quantified; for the extinction cross section and single scattering albedo, maximal changes of a few percent were observed. The phase function was shown to be different by up to twice the values derived from spherical assumptions, at large scattering angles. These results matched the predictions of previous studies and suggestions for further research in the field are given.

INDEX

1. INTRODUCTION

1.1 The problem

In order to make physical problems tractable, physicists frequently have to make approximations about the system that is being solved. The accuracy of the solutions is then limited by the degree to which the model deviates from the actual system. Even in one of the largest and highly non-linear problems of atmospheric modelling, the constituents have to be approximated. Apart from the well-known mixture of gases present in the atmosphere, it also contains water and ice particles (clouds) and aerosols, where an aerosol is any solid or liquid particulate matter larger than a molecule that can remain suspended in the atmosphere (Hess et al., 1998). There exists the underlying assumption that both the cloud particles and aerosols are perfectly spherical. In remote sensing experiments, this allows for speedy retrievals of pre-computed optical properties using the Mie-Lorentz theory of light scattering. While it is true that ice and water particles will tend to form spherical shapes due to their molecules' surface tension, for many types of aerosols this is a gross oversimplification. Many types of particulate matter little resemble spheres, instead being highly irregular aggregates of a wide range of materials (Nakajima et al., 1989). Hence, this predominantly spherical model of particle shapes may lead to large errors in the retrievals of optical properties.

1.2 Impact of aerosols on the climate

The term aerosol refers to many distinct classes of particulate matter which can either be man-made or occur naturally. Examples of man-made aerosols include sulphates and nitrates from fossil fuel combustion as well as soot and organic matter from biomass combustion. Natural aerosols can come about as results of wind-blown mineral dusts, ashes from volcanic eruptions or sea-foam spray. All aerosols play an important part in radiative transfer equations that allow scientists to model the atmosphere, as they can control the lifetime of clouds and reflect or absorb solar radiation directly. It is currently unclear what overall effect aerosols have on the energy budget of the atmosphere; there are many conflicting studies on the effects of man-made aerosols on radiative budget of the planet (Bellouin et al., 2005; Chung et al., 2005). While the climatic effects of greenhouse gases have been studied extensively and well quantified, aerosol climate effects are more complex, with large uncertainties (International Panel on Climate Change, 2001). According to Dickerson et al. (1997), aerosols can also alter the radiative balance in the atmosphere so that particulate matter such as desert dust that strongly absorbs UV radiation could drastically reduce the rate of ozone production.

1.3 The importance of desert dust as an aerosol

In some regions close to deserts, desert dust is the dominant type of aerosol (Nousiainen et al., 2006) with a rate of production ranging from 60 to 3,000 million tonnes per year worldwide (D'Almeida et al., 1991). In terms of its effects, desert dust can significantly affect direct radiative forcing on both a regional and global scale; it has also been suggested that desert dust plays a major role in regulating precipitation in dry regions (Yoshioka et al., 2006). Therefore, it is important to be able to quantify the relevant characteristics of desert dust, from remote sensing, in order that rainfall may be effectively modelled. Dust particles also affect atmospheric chemistry as they have a large surface area due to their irregular shapes and thus control many heterogeneous chemical reactions.

In addition to climatic effects, desert dust aerosols can .pose a hazard to human health. Particles with a radius below 2.5 microns can efficiently penetrate the lungs where their surface coatings, such as iron oxide contained in African dusts, can react with lung tissues to produce an inflammatory response (Prospero, 1999). Furthermore, it has been proposed that ultrafine particles with radii below 50nm, such as desert dust transported a long distance from the source, might "play a role in causing acute lung injury in sensitive parts of the population" (p111, Oberdorster et al., 1995). However, such small particulate matter is far more likely to come from local anthropogenic sources (Prospero, 1999). On the other hand, coarse particles with radii of 2.5 microns or above were shown to have no effect on human mortality rates in a study by Laden et al. (2000). Dust particles with such radii would most likely be produced locally as these larger particles would be removed from the atmosphere upon transit by gravitational settling or precipitation (Pierangelo et al., 2004).

1.4 Optical properties of aerosols

The optical properties of desert dust, like many aerosols, can be deduced from remote sensing data gathered by satellites, for instance, the Aerosol Optical Depth (AOD) can be obtained from radiance measurements. The AOD is a dimensionless parameter that specifies the amount of attenuation solar light that goes through while passing through the aerosols in the atmosphere, so that an AOD of 1 would denote solar radiation at that particular frequency is reduced by a factor of $e^{-1} \approx 0.368$ upon reaching the Earth's surface through a vertical column. Knowledge of the AOD is important as it allows us to estimate the macrophysical properties of the aerosol, such as the number density and its vertical structure in the atmosphere. Once the AOD is found at different wavelengths, the average radius of the aerosol size distribution may be found. While AODs can be readily found for clear, cloudless areas above water, determining the AODs over land is still difficult and an active area of research (Vincent et al., 2006). Another important set of optical properties that can be measured is the Scattering Matrix, of which the Phase Function (F11) is the most important; it is a dimensionless function relating the intensity of scattered light to the intensity of incident light at a given angle of scattering. The other elements of the Scattering Matrix are related to the polarisation states of the scattered light and are not used here, although they can be an important indicator of a non-

spherical particle shape (Mishchenko, 1993). Further characterisations of aerosol properties can be made with the single-scattering albedo (SSA), which is the ratio between the scattering and extinction coefficients, and defines the probability that a given photon will be scattered and not absorbed upon interacting with the aerosol. The SSA is important as the largest component of light observed at visible wavelengths is singly-scattered (Veihelmann, 2005), and is used to derive radiative forcing effects.

1.5 The Transition matrix method

Particles that scatter light such as the aforementioned aerosols can be quantified by the size parameter χ_s, given by $\chi_s = 2\pi r / \lambda$, where r is the radius of the particle and λ the wavelength of light being scattered. In terms of the size parameter, a modern method bridges the gap between Rayleigh ($\chi_s << 1$) and Geometric Optics scattering ($\chi_s > 100$): the T-matrix method. The theoretical basis for calculating optical properties for non-spherical particles has been in place for decades (van de Hulst, 1957). The problem with modelling such problems was the limited computing power available to solve the resulting equations. The modelling of scattered light by non-spherical particles progressed with Waterman's (1965, 1971) T-matrix formulation that used the Extended Boundary Condition Method. This involved numerically solving Maxwell's equations for small particles whose size was comparable to the wavelength of light in which they were observed. The technique is briefly outlined here, although a full discussion can be found in Mishchenko's (1993) paper.

The incident and scattered electromagnetic waves are expanded in vector spherical functions. The linearity of Maxwell's equations and constitutive equations implies that the relation between the scattered and incident field expansion coefficients can be given by the transition matrix (T-matrix). This T-matrix depends solely on the morphology of the particle, its size relative to the wavelength, the relative refractive index and orientation relative to the laboratory reference frame. As soon as it is computed for a particular direction, it can be used to work out the optical properties in any direction of incident or scattered waves for any polarisation state. Thus, computing orientation averaged scattering quantities from a pre-computed T-matrix is very efficient in terms of the necessary computing time. As computer technology advanced, the early 1990s saw Waterman's T-matrix method improved upon by many authors, allowing for larger size parameters in the calculations and for axisymmetric shapes other than spheroids (Mishchenko, 1991). Nonaxisymmetric particle scattering was investigated by Wriedt and Doicu (1998) who have used it to study scattering from ellipsoids and cubes. The method was extended to bispheres by Mishchenko & Mackowski (1994), to finite circular cylinders by Mishchenko et al. (1996) and hexagonal columns by Baran et al. (2001). A comprehensive review of the literature leading to improvements in the T-matrix codes can be found in Mishchenko et al. (2005).

1.6 Previous T-matrix studies

In light of the freely-available and easily-accessible T-matrix code, studies using compiled programs to study non-spherical particles have been numerous. The code is very versatile and has even been used to model the optical properties of red iron oxide pigments used in architectural paints, with some success (Auger et al., 2005).

The applicability of modelling aerosols as spheroids was tested in many studies, particularly for a sample of feldspar (a large group of rock-forming minerals that make up more than 50% of the Earth's crust) whose optical properties were thoroughly measured (Volten et al., 2001). Nousiainen et al. (2005) concluded that the best fit phase matrix came about when the feldspar particles were modelled as having a distribution of both aspect ratios and radii. The distribution was one that gave most weighting to extreme values of the aspect ratio. This was unlike the equi-probable distribution in aspect ratios previously used to model desert dust aerosols (Dubovik et al., 2002). Moreover, this extreme aspect ratio distribution led to a magnitude decrease in the error versus spherical particles in a radiative transfer model (Kahnert et al., 2005). The Dubovik et al. study had carried out computations of the optical properties of polydisperse, randomly-oriented non-spherical aerosols and compared their computed results to the AERONET (AErosol RObotic NETwork) database (discussed in detail by Holben et al. (2001)). Dubovik et al. concluded that using a spheroid model for the constituent

particles produced a better match to the measured aerosol than one using spheres only. There have been indications that using retrievals based on the spherical approximation could affect the measurement of certain atmospheric variables by as much as a factor of two (Mishchenko et al., 1995). Indeed, Veihelmann et al. (2004) have shown that using spherical models of desert dust particles may comprise large error contributions to measurements of the Aerosol Optical Depth (Zhao et al., 2003).

While the computer code provides exact solutions, given enough processing power, the output is still limited by the accuracy of the initial approximations. Modelling is complicated by the uncertainty in the refractive index of desert dust at a given wavelength, simply because of the presence of so many different compounds within a particular sample of dust. A study by Avila et al. (1997) of African dusts transported to north-eastern Spain has shown there to be at least 8 such constituents; illite, quartz, smectite, palygorskite, kaolinite, calcite, dolomite and feldspars. To further complicate matters, transported desert dust particles tend to have coatings of various oxides on their surfaces, such as iron oxide in the case of African dust (Glaccum & Prospero, 1980).

The major unresolved problems with adopting non-spherical retrievals when observing aerosols such as desert dust are the uncertainties of basic properties, particularly with regards to the value of the refractive index, although the problem exists for spherical retrievals as well. This is because there are few in-situ measurements of the optical properties of desert dust (Olmo et al., 2006). The vertical structure of desert dust aerosols is even more poorly understood (Duce, 1995). The computing requirements for calculating optical properties with the T-matrix code are still immense, especially for particle distributions that have large maximum particle radii with respect to the wavelength or have high size parameters, although these can be calculated using other numerical methods such as ray-tracing and Geometric Optics.

1.7 Outline of current study

In this study, we will attempt to quantify the difference between modelling desert dust particles as being spherical or non-spherical with moderate aspect ratios. As outlined in Mischenko et al. (1993), a large difference in the scattering and extinction coefficients or the single scattering albedo is not expected. The phase function for spherical and spheroid desert dust is, however, expected to be substantially different, especially at angles above 100°. Changes in the phase function would affect the retrieved radiances from remote sensing instruments, which are in turn used to calculate the single scattering albedo (Fraser & Kaufman, 1985; Tanré et al., 2001). In a paper by Wang et al. (2003), the remote sensing retrievals of phase functions and scattering properties were found to be greatly improved by using a mixture of both spherical and non spherical phase functions; the desert dust mixture that we are going to be modelling consists of both spherical and non-spherical particles with the associated phase functions.

2. METHOD

The FORTRAN source code for a T-matrix program was acquired, along with the source code for a program that would use Lorentz-Mie theory to obtain the scattering properties of polydisperse, randomly-oriented spherical and non-spherical particles (Mishchenko & Travis, 1998). The code was compiled for use on an x86 system using Silverfrost FTN95 for Microsoft® .NET and Win32. Both programs were modified to produce an output file containing the relevant scattering data so that it could be retrieved at any time for analysis. In particular, the phase function at each scattering angle, extinction cross section and single scattering albedo were recorded to file.

2.1 Program input

- The input parameters for both programs were as follows:

DEG - The degree separation of equidistant scattering angles (from 0° to 180°) for which the scattering matrix is calculated. A value of 0.5 was used.

NKMAX + 2 - The number of Gaussian quadrature points used in integrating over the size distribution for particles. It was observed that the phase functions that were being output by the T-matrix code were more uneven than expected

from such calculations (Mishchenko et al., 1996). A control run was therefore used where the same input variables were applied to both the T-matrix and Lorentz-Mie programs, with the expectation that both should give the same output. The results of the T-matrix program showed significant deviations from the spherical Mie phase function; the error was the abnormally small number of Gaussian quadrature points used in the T-matrix code. Upon increasing NKMAX to 50, both the Lorentz-Mie and T-matrix results were almost identical, at the expense of a higher computing time for the T-matrix program. After this calibration, the Lorentz-Mie program was used throughout in order to model the scattering characteristics of particles that were exactly spherical owing to the much lower computational time required compared to the T-matrix for the same input.

LAM - The wavelength of light in microns. The visible and short-wavelength IR instrument wavelengths of the SEVIRI satellite were used (0.640, 0.809, 1.64) as well as the reference 0.550 wavelength.

NDISTR, R1, R2, MRR, MRI - The shape of the distribution, the minimum and maximum equivalent-sphere radii in the size distribution, and real and imaginary parts of the refractive index respectively. These were taken from the OPAC database and are discussed in depth in a paper by Hess et al. (1998). The imaginary part of the refractive index is taken to be greater than 0. For all aerosol components of the atmosphere, the particles' radius distribution in number was lognormal. Conveniently, the T-Matrix and Mie codes, as well as the OPAC database use the following equation for the number distribution:

$$\frac{dN_i(r)}{dr} = \frac{N_i}{\sqrt{2\pi} r \log\sigma_i \ln 10} \exp\left[\frac{1}{2}\left(\frac{\log r - \log r_{\mathrm{mod}N,i}}{\log\sigma_i}\right)^2\right] \quad (1.1)$$

In setting the limits on the minimum and maximum radii of the distribution for use in the Lorentz-Mie and T-matrix codes, the volume distribution of the particles was useful, for which the mode radius is defined by

$$r_{\mathrm{mod}V} = r_{\mathrm{mod}N} 10^{(3\log^2(\sigma_i)\ln 10)} \quad (1.2)$$

- Furthermore, for the T-matrix code, 4 extra values are used to parameterise aspherical particles.

RAT=1, RAT≠1 – The specification of particle size in terms of the equal-volume-sphere radius or the equal-surface area-sphere respectively. The former was used throughout (Mishchenko, 1993).

NP - The shape of the particles. This was set to spheroids (NP = -1) for all further calculations (Nousiainen & Vermeulen, 2003).

NDGS - The parameter controlling the number of division points in computing integrals over the particle surface. The recommended values in the source code were 2 for compact particles, 3+ for highly aspherical particles, with an increase sometimes necessary to aid convergence of the code. This was set to 5 throughout as it did not seem to adversely affect processing time required.

EPS - The ratio of the horizontal to rotational axes. Veihelmann et al. (2004) have shown that the aspect ratios of spheroids that best match real desert dust particles lie between 0.5 and 1.8. Hence, the maximal ratio used in this study was 1.5 as this was closest to the extremal value but remained tractable in terms of computing time. However, the same study also demonstrated that the best match for realistic values of other parameters was obtained using a distribution of aspect ratios, such that the highly oblate and prolate spheroids were weighed much more heavily than moderate ratios. Limited time and computing resources meant that these extreme aspect ratios could not be modelled satisfactorily and hence were not used.

2.2 Desert dust mixtures

In order to model desert dust, one can use a particle size distribution containing one or more modes of mineral aerosols. Averaging techniques can then be used to obtain the bulk properties of the mixture. The details of the lognormal number distributions for these are reported in Table 1. One way to model this was to take combinations of the water-soluble, and 3 mineral aerosol components; accumulation (acc.), nucleation (nuc.) and coarse (coa.) mode. By changing the external mixing ratios between the components it was possible to vary the effective radius of the mixture.

Particle type	R_{min} (μm)	R_{mod} (μm)	R_{max} (μm)	σ
Water-soluble	0.006	0.0262	25	2.24
Mineral (nuc.)	0.005	0.07	20	1.95
Mineral (acc.)	0.005	0.39	20	2.00
Mineral (coa.)	0.005	1.90	60	2.15
Mineral (tra.)	0.020	0.50	5.0	2.20

***Table 1**: The defining values of lognormal distributions of 3 different components of desert dust, together with that of transported dust matter and water-soluble particles.*

For the SEVIRI satellite channels, the refractive indices for mineral aerosols were taken from the OPAC database and are reported in Table 2. The 550 nm channel is the reference wavelength for most measurements of the aerosol optical depth (Pierangelo et al., 2004).

Wavelength (nm)	Refractive Index{Re}	Refractive Index{Im}
550	1.53	0.0055
640	1.53	0.0045
809	1.53	0.0040
1640	1.53	0.0061

***Table 2**: The complex refractive indices of desert dust at various SEVIRI satellite wavelengths, along with the reference 550nm wavelength*

The extinction coefficient (σ_e) (Hess et al., 1998), single scattering albedo (ω), and phase function ($P(\theta)$) (Carboni, private communication) for the mixture of aerosols could then be calculated as shown in Equations 1.3-1.5.

$$\sigma_e = \frac{\sum_i \sigma_{e,i} N_i}{\sum_i N_i} \tag{1.3}$$

$$\omega = \frac{\sum_i \omega_i \sigma_{e,i} N_i}{\sum_i \sigma_{e,i} N_i} \tag{1.4}$$

$$P(\theta) = \frac{\sum_i P_i(\theta) \omega_i N_i}{\sum_i \omega_i N_i} \tag{1.5}$$

However, the large size parameter and the high R_{max} of the lognormal distribution for the coarse mode desert dust meant that the T-matrix code would not converge for optical wavelengths, and showed few interesting features in the IR region for which convergence could be obtained. It was not possible to physically account for a desert dust model containing only two of the above mentioned mineral aerosols or a model where the coarse mode particles were perfectly spherical.

2.3 Transported mineral dust model

The above circumstances effectively constrained the model of desert dust particles to a bimodal distribution containing only the water-soluble aerosol and mineral transport mode particles. This kind of distribution would be applicable to desert dust carried away from the source of origin with a much reduced content of large particles (Hess et al., 1998). The physical feasibility of this desert dust model was confirmed by previous studies that have shown that transported dust appeared to have far fewer large particles than at the point of origin (Maring et al., 2003; Pierangelo et al., 2004). This was attributed to a loss in coarse mode particles by gravitational settling. The OPAC refractive indices of transport mode desert dust were shown to be accurate values for modelling optical properties of far-travelling desert dust swept out of the Sahara above the Atlantic Ocean (Sokolik et al., 1998). Water-soluble aerosol components remain spherical at all times due to the surface tension of water in which they are dissolved, whereas the mineral particles remain irregularly shaped regardless of the relative humidity, at least in the case of Saharan dust (Fan et al., 2004). The optical properties of North African dust aerosols were shown to be insensitive to the relative humidity (Li-Jones et al., 1998) hence only the aspect ratio of the transport mode particles was altered, ranging from a value of 0.8 to 1.5.

Mixture ratios between the two externally mixed components were then devised such that the computed effective radius, given by Equation 1.6 (Grainger, private communication) would vary smoothly from the r_{eff} of the water soluble aerosol alone to the r_{eff} of the transport mode alone.

$$r_{eff} = \frac{\sum_i r_{\mathrm{mod},i}{}^3 N_i \exp(4.5 \ln^2 \sigma_i)}{\sum_i r_{\mathrm{mod},i}{}^2 N_i \exp(2.0 \ln^2 \sigma_i)} \tag{1.6}$$

The extinction coefficient, single scattering albedo and phase function were then plotted as a function of effective radius, in Origin (Origin v7.5885, 2006) for both the non-spherical and spherical transport mode particles.

3. RESULTS

For the bimodal distribution of desert dust, Table 3 shows the mixing ratios used in obtaining a spread of effective radii values. $N_{wa\text{-}so}$ and N_{tra} refer to the mixing ratio of the number of water soluble and transport mode mineral dust, respectively. The extinction coefficient, single-scattering albedo and phase function of spheroids with an aspect ratio (EPS) of 1.5 deviated most of all from the same calculations for spherical particles and hence are shown in the table, as opposed to those with smaller aspect ratios. While the optical properties were calculated for all SEVIRI wavelengths, the largest deviations from the spherical to the non-spherical case occurred for the largest size parameter and hence only the lowest wavelength reference 550nm band is discussed here. In the cases where the mixture had a larger proportion of transport mode particles, the differences between the distribution of spheres and spheroids with aspect ratio 1.5 were only 3% for the extinction cross section and less than 1% for the single scattering albedo.

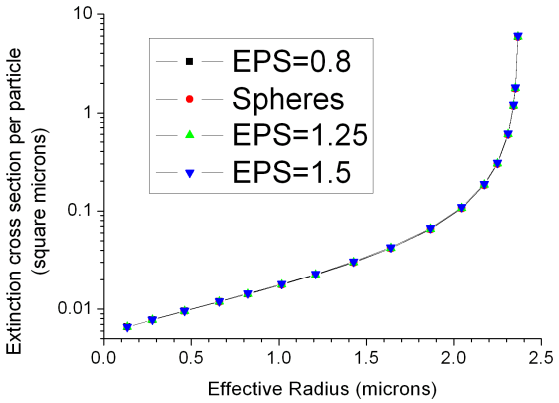

Figure 1: *The extinction cross section per particle vs. effective radius of the transported dust mixture*

The differences between the spherical and spheroid approximations to the transport mode's extinction cross section and single scattering albedo are seen to be almost negligible, and are shown in Figures 1 and 2, respectively.

Effective radius (μm)	**Mixing ratios**		**Extinction coefficient (σ_e)**			**Single-scattering albedo (ω)**		
	$N_{wa\text{-}so}$	**N_{tra}**	Spheres	Spheroids EPS=1.5	% change	Spheres	Spheroids EPS=1.5	% change
0.1332	1	0	0.0066	0.0066	0.000	0.9765	0.9765	0.000
0.2769	0.9998	0.0002	0.0078	0.0078	0.464	0.9555	0.9542	-0.138
0.4608	0.9995	0.0005	0.0095	0.0096	0.957	0.9337	0.9312	-0.264
0.6611	0.9991	0.0009	0.0118	0.0120	1.367	0.9146	0.9113	-0.359
0.8234	0.9987	0.0013	0.0142	0.0144	1.649	0.9019	0.8981	-0.415
1.0163	0.9981	0.0019	0.0177	0.0180	1.938	0.8891	0.8849	-0.465
1.2094	0.9973	0.0027	0.0224	0.0229	2.176	0.8782	0.8738	-0.501
1.4280	0.996	0.004	0.0300	0.0307	2.404	0.8679	0.8632	-0.532
1.6397	0.994	0.006	0.0417	0.0428	2.595	0.8593	0.8545	-0.553
1.8665	0.99	0.01	0.0651	0.0669	2.771	0.8514	0.8465	-0.569
2.0442	0.983	0.017	0.1061	0.1091	2.891	0.8459	0.8410	-0.579
2.1737	0.97	0.03	0.1821	0.1875	2.971	0.8423	0.8374	-0.585
2.2487	0.95	0.05	0.2992	0.3082	3.015	0.8404	0.8354	-0.588
2.3086	0.9	0.1	0.5918	0.6098	3.048	0.8389	0.8339	-0.590
2.3399	0.8	0.2	1.1769	1.2130	3.065	0.8381	0.8331	-0.591
2.3505	0.7	0.3	1.7621	1.8162	3.071	0.8378	0.8329	-0.591
2.3656	0	1	5.8584	6.0388	3.079	0.8375	0.8325	-0.592

Table 3: *The effective radius at each mixing ratio used and the associated extinction coefficient and single-scattering albedo for spheres and spheroids with aspect ratio (EPS) of 1.5, at 550nm*

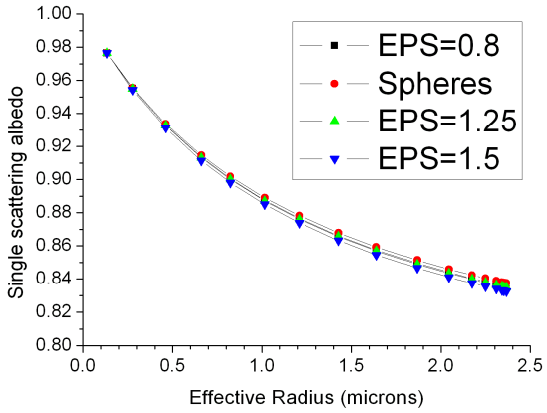

***Figure 2**: The single scattering albedo vs. the effective radius of the transported desert dust mixture*

The phase functions of spheres and spheroids, however, show clear differences for the transport mode, as illustrated in Figure 3. The most significant change in the phase function F11 occurs for angles over 120°; the proportion of light backscattered decreases as the aspect ratio is increased at angles above 160°.

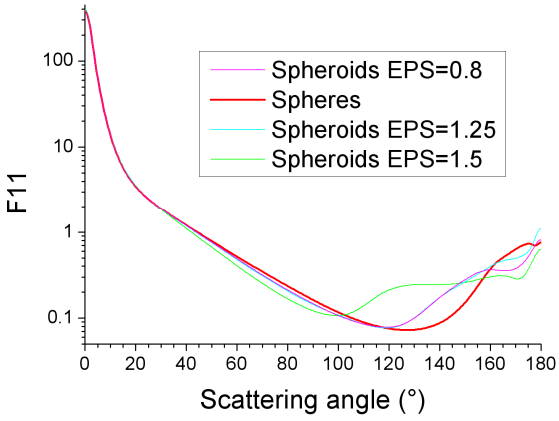

***Figure 3**: The phase function F11 of transported mineral dust vs. scattering angle, showing the difference between various aspect ratios*

A noticeable difference is seen when comparing the combined phase functions for spherical (Figure 4) and non-spherical particles (Figure 5) with aspect ratio 1.5 for the same mixing ratios. The coloured lines correspond to different values of the effective radius, R_{eff}. The biggest changes in F11 occur for the largest effective radii values i.e. as the mixing ratio of the transport mode is increased. Furthermore, there is much more forward scattering as the proportion of transport mode particles increases.

If a Lorentz-Mie model is assumed throughout the two modes, the phase function is overestimated at angles $10° < \theta < 110°$, and is underestimated for angles above 110°. The largest difference occurs at the backscattering angles above 160°, as shown in the insets of both Figures 4 and 5. Here the phase function for spheroids may be smaller than the phase function for spheres by more than a factor of two.

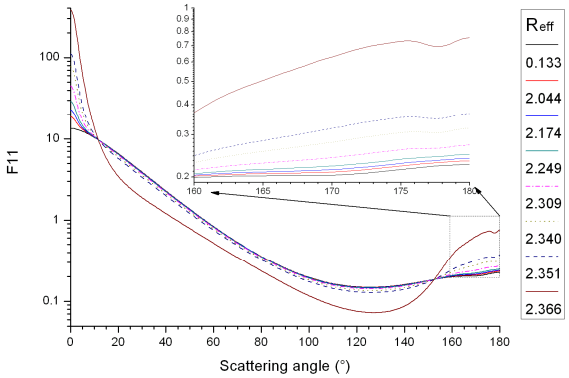

***Figure 4**: The combined phase function F11 vs. scattering angle for both spherical water soluble and transported mineral dust particles*

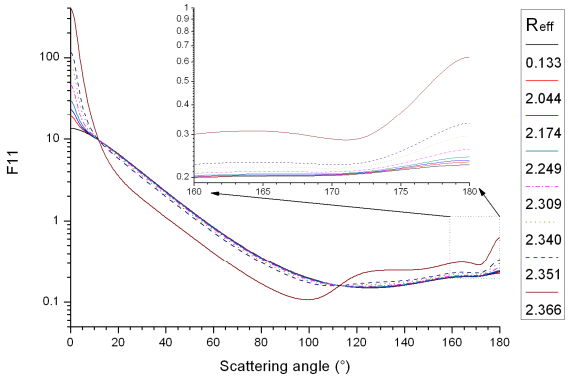

***Figure 5**: The combined phase function F11 vs. scattering angle for spherical water soluble and transported mineral dust particles with an EPS of 1.5*

4. DISCUSSION

Maximal changes of 0.5-3% were observed in the extinction cross section and single scattering albedo using a spherical and non-spherical model, but the phase function was shown to be different by up to twice the values derived from spherical assumptions. The lack of a significant difference in the extinction and scattering coefficients and ω between spheres and spheroids could be attributed

to the small size parameter of the transport mode particles and the fact that our desert dust mixtures contained significantly more spherical water-soluble particles than transport so that there was a greater range of effective radii values. The uncertainty in the value of the refractive index for the components of the mixture would not have a great effect on the output, within sensible limits, as discussed in Mishchenko et al. (1995). From the geometry of remote sensing satellite measurements, the most important regions are the backscattering ones i.e. angles above 90°. It is here, or specifically above 110° that we see the phase function being underestimated for the case of spheroid transport mode particles. These differences in phase function compare well with research by Zhao et al. (2003) and Mishchenko et al. (1995). The fact that there was much more forward scattering as the proportion of transport mode particles increased is simply the result of diffraction in the larger particles of desert dust.

A desert dust mixture proposed by Hess et al. (1998) consists of the water soluble aerosols having a mixing ratio of 0.87, with 3 mineral dust components having the remaining 0.13. If the 3 components are taken to be equivalent to the transport mode described above, this roughly corresponds to an effective radius of 2.31 microns, illustrated by the green curve in Figures 4 and 5. The aerosol optical depth, retrieved from backscattered solar radiance, is proportional to $[\omega P(\theta)]^{-1}$, hence the fact that the spheroid phase function was calculated as being smaller at angles above 160° than for the spheres meant that the aerosol optical depth could have been underestimated by a factor of two for those observing angles for the proposed desert dust mixture. This is clearly a large difference in pinning down the value of an important atmospheric variable. The AOD can be calculated by multiplying the extinction coefficient, which is a standard output of the T-matrix code, by the total number of particles. (Pierangelo et al., 2004)

4.1 Further study

While our predictions have borne out for a model of desert dust lacking large particles, it would nonetheless be instructive to repeat the above calculations with a model of desert dust directly above the source i.e. one containing accumulation, nucleation and coarse modes. The coarse mode particles are likely to affect the results significantly due to their larger size compared to the visible wavelengths (Mishchenko et al., 1993). The optical properties of these larger particles could effectively be calculated with the geometric-optics-integral-equation, as was done for aerosols in Dubovik et al. (2002). Using a distribution of aspect ratios for the spheroids such that the extremal values were heavily weighted would also be a possible avenue for further study, as this was shown to increase the accuracy of optical data retrievals more than using an equi-probable distribution (Veihelmann et al., 2004). Mishchenko et al. (1994) have proposed that using highly deformed spheres in random orientations effectively allows the distribution of them to be have a smaller spread around the mode due to averaging effects. In terms of further research, this would reduce calculation time that would be quite high for such extreme aspect ratios.

North African desert dust is a good starting point for modelling mineral aerosol particles but there are many more types of desert dust in other regions of the world. For example, dust over the Pacific is significantly more hydrophilic than its Saharan counterpart due to accumulation of pollutants on its surface (Fan et al., 2004) and is hence expected to achieve a more spherical shape in high humidity. Such effects also need further study.

5. CONCLUSION

This study sought to quantify the effects of non-sphericity of desert dust transferred away from its source, on remote sensing retrievals. Whilst similar research has been carried out into desert dust mixtures close to the mineral source, this study addressed desert dust aerosols that are transported a long distance away by wind, such as North African mineral particles swept across the Atlantic Ocean. Optical properties for a bimodal distribution of transported desert dust consisting of spherical water-soluble particulate matter and mineral dust were calculated using a T-matrix program. The results do not deviate from those found in previous studies of the general effect of non-sphericity on observed optical properties (Mischenko et al., 1993; Dubovik et al., 2002). This study confirms that the phase function for the studied bimodal model may be over or under-

estimated by as much as a factor of 2 for the largest size parameters used, specifically at scattering angles over 110°. This in turn has important consequences for the retrieval of the aerosol optical depth and its derived quantities.

Acknowledgements

The author would like to thank Dr Elisa Carboni for always taking the time to offer helpful guidance throughout the project, and Dr Michael Mishchenko for providing the T-matrix and Lorentz-Mie scattering source codes.

REFERENCES

Auger, J., Martinez, V., & Stout, B., 2005, *Scattering and absorption efficiencies of arbitrary-shaped iron oxide pigments*, 8th Conference on Electromagnetic and Light Scattering by Nonspherical Particles: Theory, Measurements and Applications, 21-24.

Avila, A., Queralt-Mitjans, I., & Alarco´n, M., 1997, *Mineralogical composition of African dust delivered by red rains over northeastern Spain*, Journal of Geophysical Research 102(D18), 21977–21996.

Baran, A. J., Yang, P., & Havemann, S., 2001, *Calculation of the single-scattering properties of randomly oriented hexagonal ice columns: a comparison of the T-matrix and the finite-difference time-domain methods*, Applied Optics, 40 (24).

Bellouin, N., Boucher, O., Haywood, J., & Reddy M. S., 2005, *Global estimate of aerosol direct radiative forcing from satellite measurements*, Nature, 438, 1138– 1141.

Chung, C. E., Ramanathan, V., Kim, D. & Podgorny, I. A., 2005, *Global anthropogenic aerosol direct forcing derived from satellite and groundbased observations*, J. Geophys. Res., 110, D24207.

d'Almeida, G. A., Koepke, P. & Shettle, E. P., 1991, *Atmospheric Aerosols: Global Climatology and Radiative Characteristic,* A. Deepak Publishing, pp561.

Dickerson, R. R., Kondragunta, S., Stenchikov, G., Civerolo, K. L., Doddridge, B. G., & Holben, B. N., 1997, *The impact of aerosols on solar ultraviolet radiation and photochemical smog*, Science 278: 827–830.

Dominick, A., Vincent, N. P. S., Monterey, C. A., & Durkee, P. A., Nielsen, K. E., Zhang, J., & Reid, J. S., 2006, *Aerosol optical depth retrievals from high-resolution commericial satellite imagery over areas of high surface reflectance*, 14th Conference on Satellite Meteorology and Oceanography P3.12.

Dubovik, O., Holben, B. N., Lapyonok, T., Sinyuk, A., Mishchenko, M. I., Yang, P. & Slutsker, I. 2002, *Non-spherical aerosol retrieval method employing light scattering by spheroids*, Geophys. Res. Lett., 29(10), 1415.

Duce, R., 1995, *Sources, distributions, and fluxes of mineral aerosols and their relationship to climate*, in Dahlem Workshop on Aerosol Forcing of Climate, edited by R. J. Charlson and J. Heintzenberg, pp. 43–72, Berlin.

Fan, S., Horowitz, L. W., Levy, H. I. I. & Moxim W. J., 2004, *Impact of air pollution on wet deposition of mineral dust aerosols*, Geophys. Res. Lett. 31 L02104.

Fraser, R. S., & Kaufman, Y. J., 1985, *The relative importance of aerosol scattering and absorption in remote sensing*, IEEE J. Geosci. Remotes. Sens, 23, 525–633.

Glaccum, R. A. & Prospero, J. M., 1980, *Saharan aerosols over the tropical North Atlantic – Mineralogy*, J. M. Mar. Geol. 37, 295–321,

Hess, M., Kopke, P., & Schult, I., 1998, *Optical properties of aerosols and clouds: the software package OPAC*, Bull. Am. Meteorological Soc., 79, 831-844.

Holben, B. N., Tanré, D, Smirnov, A., et al., 2001, *An emerging ground based aerosol climatology: aerosol optical depth from AERONET*. J. Geophys. Res. 106, 12067-12097.

Kahnert, M., Nousiainen, T., & Veihelmann, B., 2005, *Spherical and spheroidal model particles as*

an error source in aerosol climate forcing and radiance computations: A case study for feldspar aerosols, J. Geophys. Res., 110, D18S13.

Laden, F., Neas, L.M., & Dockery D. W., et al., 2000, *Association of fine particulate matter from different sources with daily mortality in six U.S. cities*. Environ. Health Perspect. 108:941–947.

Li-Jones, X., & Prospero, J. M., 1998, *Variations in the size distribution of nonsea- salt sulfate aerosol in the marine boundary layer at Barbados: Impact of African dust*, J. Geophys. Res., 103(D13), 16,073– 16,084.

Maring, H., Savoie, D., Izaguirre, M., Custals, L., & Reid, J. S., 2003, *Mineral dust aerosol size distribution change during atmospheric transport*, J. Geophys. Res., 108, 8592.

Mishchenko M. I. & Travis, L. D., 1998, *Capabilities and limitations of a current FORTRAN implementation of the T-matrix method for randomly oriented, rotationally symmetric scatterers*, J. Quant. Spectrosc. Radiat. Transfer, 60, 309.

Mishchenko M. I., & Travis, L. D., 1994, *T - matrix computations of light scattering by large spheroidal particles.* Opt Commun; 109: 16–21.

Mishchenko, M. I., & Mackowski, D. W., 1994, *Light scattering by randomly oriented bispheres*, Opt. Lett. 19, 1604.

Mishchenko, M. I., 1991, *Light scattering by randomly oriented axially symmetric particles,* J. Opt. Soc. Amer., 8, 871-882.

Mishchenko, M. I., 1993, *Light scattering by size-shape distributions of randomly oriented axially symmetric particles of a size comparable to a wavelength,* Appl. Opt., 32, 4652-4666.

Mishchenko, M. I., Lacis, A. A., Carlson, B. E., & Travis, L. D., 1995, *Nonsphericity of dust-like tropospheric aerosols: Implications for aerosol remote sensing and climate modeling*, Geophys. Res. Lett., 22 (9), 1077-1080.

Mishchenko, M. I., Travis, L. D. & Macke, A., 1996, *Scattering of light by polydisperse randomly oriented finite circular cylinders*, Appl. Opt., 35 (24), 4927.

Mishchenko, M. I., Travis, L. D., & Mackowski, D. W., 1996, *Tmatrix computations of light scattering by nonspherical particles. A review*, J. Quant. Spectrosc. Radiat. Transfer 55**,** 535–575.

Mishchenko, M. I., Videen, G., Babenko, V. A., Khlebtsov, N. G. & Wriedt, T., 2004, *T-matrix theory of electromagnetic scattering by particles and its applications: a comprehensive reference database,* Journal of Quantitative Spectroscopy & Radiative Transfer, 88; 357–406.

Nakajima, T., Tanaka, M., Yamano, M., Shiobara, M., Arao, K., & Nakanishi, Y., 1989, *Aerosol optical characteristics in the yellow sand events observed in May, 1982 at Nagasaki—Part II. Models*, J. Meteor. Soc. Japan, 67, 279–291.

Nousiainen, T., & Vermeulen, K., 2003, *Comparison of measured single-scattering matrix of feldspar particles with T -matrix simulations using spheroids*. JQSRT;79/80:1031–42.

Nousiainen, T., Kahnert, M. & Veihelmann, B., 2005, *Light scattering modeling of small feldspar aerosol particles using polyhedral prisms and spheroids*, J. Quant. Spectrosc. Radiat. Transfer, in press.

Nousiainen, T., Kahnert, M., & Veihelmann, B., 2006, *Light scattering modeling of small feldspar aerosol particles using polyhedral prisms and spheroids*, J. Quant. Spectrosc. Radiat. Transfer 101, 471-487.

Oberdörster, G., 2001, *Pulmonary effects of inhaled ultrafine particles*, Int Arch Occup Environ Health. 74:1–8.

Olmo, F. J., Quirantes, A., Alcántara, A., Lyamani, H., & Alados-Arboledas, L., 2006, *Preliminary results of a non-spherical aerosol method for the retrieval of the atmospheric aerosol optical properties*, Journal of Quantitative Spectroscopy and Radiative Transfer: 100, 305-314.

Pierangelo, C., Ch´edin, A., Heilliette, S. Jacquinet-Husson, N., & Armante, R., 2004, *Dust*

altitude and infrared optical depth from AIRS, Atmos. Chem. Phys., 4, 1813-1822.

Prospero, J. M., 1999, *Assessing the impact of advected African dust on air quality and health in the eastern United States*, Hum. Ecol. Risk Assess. 5(3), 471–479.

Sokolic, I. N., Toon, O. B., & Bergstrom, R. W., 1998, *Modeling of radiative characteristics of airborne mineral aerosols at infrared wavelengths*, J. Geophys. Res., 103, 8813– 8826.

Tanré, D. Kaufman, Y. J., Holben, B. N., et al., 2001, *Climatology of dust aerosol size distribution and optical properties derived from remotely sensed data in the solar spectrum*, J. Geophys. Res. 106, 18205-18218.

Tom, X. P., Zhao, I. L., Dubovik, O, Brent, N., Holben, J. S., Tanré, D., & Pietras, C., 2003, *A study of the effect of non-spherical dust particles on the AVHRR aerosol optical thickness retrievals*, Geophysical Research Letters, 30 (6), 1317

van de Hulst, H. C., 1957, *Light Scattering by Small Particles*, Wiley, New York, pp470.

Veihelmann B, Volten H, & van der Zande W. J., 2004, Light reflected by an atmosphere containing irregular mineral dust aerosol, Geophys Res Lett; 31: L04113.

Veihelmann, B., 2005, Thesis: Sunlight on atmospheric mineral aerosol and water vapor: modeling the link between laboratory data and remote sensing, Radboud University of Nijmegen.

Volten, H., Minoz, O., Rol, E., de Haan, J., Vassen, W., & Hovenier, J., 2001, *Laboratory measurements of scattering matrices of irregular mineral particles*, J. Geophys. Res., 106, 17,375–17,401.

Wang, J., Christopher, S. A., Reid, J. S., Maring, H., Savoie, D., Livingston, J., Russell, P., Holben, B. N., & Yang, S. K., 2003, *GOES-8 retrieval of dust aerosol optical thickness over the Atlantic Ocean during PRIDE,* J. Geophys. Res., in press.

Waterman, P. C., 1965, Proc. IEEE 53, 805.

Waterman, P. C., 1971, *Symmetry, unitarity, & geometry in electromagnetic scattering,* Phys Rev D, 3: 825.

Wriedt, T., & Doicu, A., 1998, *Formulations of the extended boundary condition method for three-dimensional scattering using the method of discrete sources,* J Mod Opt; 45: 199–213.

Yoshioka, M., Mahowald, N. M., Conley, A. J., Collins, W. D., Fillmore, D.W. Zender, C. S. & Coleman, D. B., 2006*, Impact of desert dust radiative forcing on Sahel precipitation: Relative importance of dust compared to sea surfaec temperature variations, vegetation changes, and greenhouse gas warming*, J. Climate, submitted.